



HAL
open science

Aluminum combustion in wet and dry CO₂: Consequences for surface reactions

Vincent Sarou-Kanian, Jean-Claude Rifflet, Francis Millot, Iskender Gökalp

► **To cite this version:**

Vincent Sarou-Kanian, Jean-Claude Rifflet, Francis Millot, Iskender Gökalp. Aluminum combustion in wet and dry CO₂: Consequences for surface reactions. *Combustion and Flame*, 2006, 145 (1-2), pp.220-230. 10.1016/j.combustflame.2005.10.014 . hal-00429424

HAL Id: hal-00429424

<https://hal.science/hal-00429424>

Submitted on 2 Dec 2021

HAL is a multi-disciplinary open access archive for the deposit and dissemination of scientific research documents, whether they are published or not. The documents may come from teaching and research institutions in France or abroad, or from public or private research centers.

L'archive ouverte pluridisciplinaire **HAL**, est destinée au dépôt et à la diffusion de documents scientifiques de niveau recherche, publiés ou non, émanant des établissements d'enseignement et de recherche français ou étrangers, des laboratoires publics ou privés.

Aluminum combustion in wet and dry CO₂: Consequences for surface reactions.

V. Sarou-Kanian^{1,2,@}, J.C. Rifflet¹, F. Millot¹, and I. Gökalp²

¹ CNRS/CRMHT, 1D avenue de la Recherche Scientifique 45071 Orléans Cedex 2, France.

² CNRS/LCSR, 1C avenue de la Recherche Scientifique 45071 Orléans Cedex 2, France.

@ to whom correspondence should be addressed (sarou@cnrs-orleans.fr).

Full-length article

Short running title: Aluminum Combustion in Wet and Dry CO₂

Abstract

The combustion of aluminum droplets in wet (3% mol H₂O) and dry CO₂ is studied in order to identify the influence of the two atmospheres on the surface processes. Millimeter sized samples are maintained contactless in an aerodynamic levitation system and are heated continuously during burning by a laser. Ignition and combustion of the aluminum droplet are observed with a high-speed camera, the Al surface temperature is measured by an optical pyrometer, and unburnt residues are analyzed by X-ray diffraction. The determination of the burning rates and of the droplet temperatures reveals no differences between wet and dry CO₂ ($\beta=1.28\pm 0.05$ mm²/s, $T=2600\pm 50$ K), which shows that the gas-phase combustion regime is not affected by the presence of water vapor. However, the oxide cap, initially formed by the oxide coating breakdown at ignition, is progressively removed in wet CO₂, whereas it is unvarying in dry CO₂. Comparison between Al burning in CO₂/H₂ and in CO₂/(Ar or He) demonstrates that the oxide cap regression in wet atmosphere is related to a chemical effect of hydrogen produced in the flame, then diffusing and reacting at the droplet surface. It is suggested that the adsorption mechanism of H₂ on the Al surface may slow down the contribution of adsorbed oxygen containing species (CO) to the oxide cap, which would consequently promote its decomposition (=removal). Furthermore, the carbon dissolution process is observed in wet and dry CO₂. When the carbon concentration reaches the saturation limit in the burning Al droplet ($x_C=0.23$ at $T=2600$ K), the excess of carbon is ejected at the surface and forms a solid coating. In the absence of the oxide cap (=wet CO₂), the refractory carbon coating prevents strong surface oxidation, and the combustion definitely stops. In the presence of the oxide cap (=dry CO₂), the carbon coating reacts and produces an oxycarbide phase which is melted by the laser heating; a new burning regime occurs mainly controlled by direct surface reactions, and leading to the slow oxidation of the droplet and the expulsion of

dissolved carbon into CO. Finally, a qualitative model of the combustion of aluminum in CO₂ atmospheres is proposed.

Keywords: aluminum, combustion, wet and dry CO₂, surface reactions, carbon dissolution, oxide cap.

1 Introduction

Aluminized solid propellants are mainly used in the rocket boosters for heavy-lift launchers such as *Ariane 5* (MPS-230) or the *Space Shuttle* (SRB). Because of its high energetic properties, aluminum powder allows a significant increase of the specific impulse of the propellant. For this reason, the combustion of aluminum particles has been strongly studied for these last forty years [1,2]. However, some phenomena are not yet clearly understood such as the existence of an oxide cap on the Al surface [1-9], or possible fragmentation of the aluminum particle [1,3,4,9-14]. These unsteady processes mainly result from heterogeneous reactions between the gas-phase and the aluminum particle.

The oxide cap evolution is particularly related to the nature of the gaseous atmosphere. The oxide accumulation on the Al surface is generally considered resulting from the retro-diffusion of gaseous aluminum oxides (AlO, Al₂O) from the flame to the particle [15,16]. It was also observed that the presence of nitrogen promotes the oxide cap formation, while the addition of inert gases (Ar, He) seems to inhibit it [3,17,18]. In [2,19], it was shown that the oxide cap size decreases during Al burning in water containing atmospheres; an oxide cap regression rate was estimated in analogy to the burning rate, and was correlated with the droplet temperature suggesting a chemical decomposition process of alumina by liquid aluminum into gaseous species.

Apart from the oxide cap, other phases may appear on the Al surface such as the formation of aluminum nitride (AlN) and oxynitride (AlON) during the combustion in N₂ containing atmospheres [2]. The dissolution process of oxygen and carbon inside the particle is also significant. The quantities dissolved in the unburnt residue can reach about 8-10% mol O, and 18-23% mol C [18,19,20]. In fact, the carbon concentration corresponds to the carbon saturation limit in liquid aluminum. It was also found that the excess of dissolved carbon resulting from the permanent consumption of the Al particle is finally ejected at the surface.

This carbon coating prevents Al vaporization and stops the gas-phase burning [19]. However, in solid propellant conditions, as aluminum burns in hot gases ($T > 2500$ K), surface reactions may still occur even if there is no more gas-phase combustion. Such a new combustion regime could involve some of the mentioned unsteady processes (fragmentation).

In [19], we have especially studied the combustion of Al droplets in $\text{CO}_2/\text{H}_2\text{O}$ mixtures because both gases correspond to the main oxidizers produced during the solid propellant decomposition ($x_{\text{H}_2\text{O}} \approx 0.4-0.5$, $x_{\text{CO}_2} \approx 0.1$). Although high CO_2 concentrations were examined (up to 97% $\text{CO}_2 = \text{wet CO}_2$), Al burning in pure CO_2 (=dry CO_2) was not studied. Obviously, it could be considered that the combustion in wet or dry CO_2 is the same, but Prentice [4] observed that the presence of small amounts of water vapor promote fragmentation in comparison to dry gases. In addition, new propulsion systems using metals burning in pure CO_2 have been recently proposed for Mars mobility or sample return missions [21].

In the present work, the combustion of aluminum droplets in dry and wet CO_2 is investigated in order to clarify the similarities and the differences for both atmospheres. Furthermore, the existence of the second combustion regime suggested by [19] is examined. Accordingly, an experimental set-up which has been developed to observe millimeter sized aluminum droplets burning in cold gases is used to simulate the hot atmospheres in solid propellant conditions by a permanent laser heating. Analyses of the surface phenomena occurring during the combustion and examinations of the unburnt residues are performed and a new qualitative model of the Al burning in CO_2 atmospheres is proposed.

2 Experimental

The experimental set-up was detailed previously [2,19]. A 3-millimeter aluminum droplet is maintained contactless in an aerodynamic levitation system and is heated by a continuous CO_2 laser. Levitation gases are used as the oxidizing environment; for the wet atmosphere, CO_2 is

saturated with H₂O vapor by flowing it through a water bath at ambient temperature. For these conditions, wet CO₂ does not contain more than 3% mol H₂O. The ignition and combustion processes are analyzed both with a high-speed CCD camera (*Kodak EktaPro 1000HRCOLOR*, 250-1000 frames/s, optical magnification about 1), and with a monochromatic optical pyrometer ($\lambda \approx 0.8 \mu\text{m}$) aiming the bottom hemisphere of the droplet for which we have a clear view of the surface, the oxide smokes being continually ejected in the upper wake of the flame by the levitation gas flow.

As it was shown in [19] with the same experimental set-up, the combustion of aluminum droplets is not self-sustaining for high CO₂ concentrations in H₂O/CO₂ mixtures ($x_{\text{CO}_2} > 0.8$) when the laser is cut off. In the present work, in order to observe the second combustion regime which may begin after the carbon ejection at the droplet surface, the laser keeps on heating all along the burning process with a minimum laser power (at ignition, typically $P = 150\text{-}200 \text{ W}$; during burning $P_{\text{min}} = 50\text{-}70 \text{ W}$).

Some unburnt residues are also analyzed by X-Ray diffraction. They concern burning Al droplets which have cooled down slowly after the laser is cut-off, without fragmentation or violent impact on the levitation nozzle, and which have produced crystallized phases.

3 Results

3.1 Observations with the camera

The first stage of Al droplet combustion was already described in [2,19]. The preheating phase corresponds to a partial oxidation of the droplet surface (Figure 1:Frames 1); a thin solid coating gradually grows (thickness $< 10 \mu\text{m}$) and prevents any burning at low temperature. Ignition occurs when the oxide coating breaks (Frames 2) and liquefies as a single oxide cap. Aluminum starts to vaporize, and burns in a diffusion flame regime far from

the droplet surface. Then steady state gas-phase burning sets in with the regression of the droplet size (Frames 3-6). However, there is a significant difference between wet and dry CO₂ concerning the oxide cap. In wet CO₂, its size decreases until complete disappearance, when it seems unvarying in dry CO₂. This is a crucial point because the presence or the absence of the oxide cap deeply modifies the carbon ejection process and the nature of the second burning regime.

In wet CO₂ (Figure 2: Frames 1-4), carbon suddenly appears at the surface and covers entirely the droplet in few milliseconds ($t < 30$ ms). This carbon coating prevents Al vaporization, and marks the end of the gas-phase burning. At this stage, although the laser keeps on heating the droplet, there are no surface reactions with the gaseous environment (Frames 5-6). The top hemisphere of the droplet is overheated, but the carbon coating guarantees an efficient protection from high oxidation. Nevertheless, for some experiments, the expulsion (Frames 7-9) or the expulsion attempt (Frames 10-16) of small Al satellites from the inside of the droplet is also observed. This phenomenon is not considered as fragmentation because the integrity of the initial droplet is not affected. Indeed, a new coating rapidly covers the zone where the expulsion occurred (Frames 9-10); in the case of an aborted attempt (Frames 15-16), the satellite is absorbed back, and the surface remains protected by the carbon coating.

In dry CO₂ (Figure 3), small carbon islands first appear on the droplet surface (Frame 1) and grow more slowly than in wet CO₂ ($t > 0.5$ s, Frames 2-5). While this phase has not surrounded the oxide cap (Frame 6), the interactions between the two objects are not really significant; no ingestion process occurs such as between AlN and Al₂O₃ [2]. But at the complete covering (end of gas-phase burning/start of second regime), the cap and the carbon phase being in contact, the laser beam succeeds in melting the coated surface in the top hemisphere of the droplet (Frames 7-9). Small caps are formed continuously, coalesce and solidify again in the bottom hemisphere (no laser). The overheated top hemisphere allows new vaporization of

aluminum and the formation of a local flame zone. In most experiments, the droplet suddenly presents intense deformations, its volume strongly increases (Frames 10-16), and sometimes fragmentation occurs (Figure 4). This phenomenon is very fast and violent ($t < 20$ ms) and generally causes the impact of the droplet on the walls of the levitator and the end of burning. For some experiments without fragmentation in dry CO_2 , the droplet was heated again several times. The first heating are similar to the second burning regime described previously (partial liquefaction of the coating – Al vaporization and located flame). Then the droplet surface completely changes (Figure 5) with only bubbles appearing, coalescing, and finally breaking up. It is also noted that the gases escaping from these bubbles do not react with the ambient atmosphere.

3.2 Pyrometric measurements

Figure 6 illustrates pyrometric signals for aluminum droplets burning in wet and dry CO_2 . Here $t=0$ s is arbitrary and does not correspond to the laser start; the preheating duration is longer ($t > 10$ s) and is different for each experiment. In fact, it depends both on the laser power, and on the oxide coating thickness and roughness. As a result, the intensity of the signal at ignition may vary as in the present figure. But, when the combustion begins, the two signals rapidly increase and reach the same steady value all along the gas-phase burning (plateau). Then, there is a sudden increase of signal (1) related to the appearance of the solid and liquid phases at the droplet surface which are more emissive than aluminum (Figure 2 and Figure 3). In dry CO_2 , the small peaks (2) correspond to the beginning of the carbon ejection, the surface covering being slower than in wet CO_2 . In Figure 6, the carbon ejection occurs sooner in dry CO_2 than in wet CO_2 ; this observation is a general trend between the two atmospheres.

The optical pyrometer is first calibrated using the crystallization plateau of a liquid alumina droplet ($T=2327$ K) freely cooling in the same experimental conditions (same droplet size and

gaseous atmospheres) as in the burning ones [22]. The temperature measurement is deduced from the Wien's approximation of the second Planck's law, and the assumption that the droplet surface is a grey-body ($\epsilon_\lambda < 1$). It is expressed such as:

$$\frac{1}{T_{\text{exp}}} = \frac{1}{T_{\text{cal}}} + \frac{\lambda}{C_2} \cdot \text{Ln} \left(\frac{\epsilon_{\text{exp}} \cdot U_{\text{cal}}}{\epsilon_{\text{cal}} \cdot U_{\text{exp}}} \right) \quad (1)$$

with T , ϵ , and U respectively the temperature, the spectral emissivity at wavelength λ ($=0.8 \mu\text{m}$), and the pyrometric output voltage, for Al burning experiments (subscript "exp") and for calibrations with alumina (subscript "cal"). C_2 ($=14388 \mu\text{m.K}$) represents the second radiation constant.

For the monochromatic pyrometry technique, the emissivity ratio $\epsilon_{\text{exp}}/\epsilon_{\text{cal}}$ has to be fixed. This point was already discussed in [19], and $\epsilon_{\text{exp}}/\epsilon_{\text{cal}} = 0.30 \pm 0.03$ is chosen especially for the gas-phase combustion (no surface coating). During the steady burning process (plateau), the droplet surface is $2600 \pm 50 \text{ K}$, and agrees with [19] for Al burning experiments in $\text{H}_2\text{O}/\text{CO}_2$ mixtures when the laser was cut off. This shows that the laser contribution with the minimum power is only used to maintain steady state burning and not for overheating. When the solid and liquid phases appear on the droplet surface, no temperature measurements can be accurately performed because the emissive properties of such coatings are difficult to estimate. Nevertheless, it may be reasonably assumed that $\epsilon_{\text{gas-phase}} < \epsilon_{\text{coating}} < \epsilon_{\text{Al}_2\text{O}_3}$, that is $2400 < T < 2700 \text{ K}$ during the second combustion regime.

3.3 Regression rates

As shown in Figure 1, the dimensions of the Al droplet and of the oxide cap during the gas-phase burning can be easily deduced from the images recorded by the high-speed camera. The Al droplet is assumed spherical, and the measure of its projected surface provides the squared diameter value (uncertainty $< 5\%$). For the oxide cap, only its circular basis is evaluated. Even if its projection is generally an ellipse, the major axis always corresponds to the radius of the

projected circle. Figure 7 illustrates the evolution of the reduced squared diameter versus the reduced time for burning droplet in wet and dry CO₂. It is observed that there are no differences between the two atmospheres. The average burning rates (slopes of the linear regression) are $\beta_{\text{dry}}=1.28\pm 0.05$ mm²/s and $\beta_{\text{wet}}=1.29\pm 0.05$ mm²/s. Note that these burning rates are obtained under forced convection [2,19]; their corresponding values under stagnant atmosphere are not indicated here because the correction factors (deduced from Nusselt and Sherwood numbers correlated to Reynolds, Prandtl and Schmidt numbers) are the same for wet and dry CO₂ and does not change the comparison. Figure 8 shows the opposite behavior for the oxide caps between wet and dry CO₂. As introduced previously in 3.1., the oxide cap size decreases until disappearance in wet CO₂, when it is quite constant or slightly decreasing in dry CO₂. The average oxide cap regression rates are $K_{\text{wet}}=0.33\pm 0.03$ mm²/s and $K_{\text{dry}}<0.1$ mm²/s.

3.4 Unburnt residues

The X-Ray diffraction analysis was carried out for some unburnt residues in wet and, more particularly, in dry CO₂. As summarized in Table I, the crystallized phases found in the residues are metallic aluminum (Al), alumina (α -Al₂O₃), aluminum carbide (Al₄C₃), and aluminum oxycarbide (Al₄O₄C). In wet and dry CO₂, the residues with no reheat mostly contain Al and Al₄C₃, and significant amounts of Al₄O₄C. But when the residues are heated again (only in wet CO₂), the quantities of the oxygen containing phases (Al₄O₄C and Al₂O₃) become more and more important as heating times increase. At the final stage of burning with bubbles breaking up at the droplet surface (Figure 5), there are no more Al and Al₄C₃, Al₄O₄C finally disappears, and only Al₂O₃ is detected.

4 Discussion

The present results have pointed out the similarities (gas-phase) and the differences (surface phenomena) between wet and dry CO₂ for the combustion of aluminum droplets.

4.1 Gas-Phase

The gas-phase burning is unvarying for both atmospheres. Indeed, the burning rates and the droplet temperatures characterizing this process are the same (respectively $\beta \approx 1.28 \text{ mm}^2/\text{s}$, $T \approx 2600 \text{ K}$). Prentice [4] showed that the burning times of submillimetric Al particles were slightly higher in dry mixtures (O₂/Ar, O₂/N₂, CO₂/O₂) than in wet ones. In fact, it must be considered that the reaction $\text{Al}_g + \text{H}_2\text{O}$ in the flame yields to hydrogen which has better transport properties (molecular and thermal diffusion – light gas) than any other gaseous products such as CO. Accordingly, the presence of H₂ between the droplet and the flame promotes the diffusion of the Al vapor that allows increasing the burning rate [19]. In the present experiments, the amounts of water vapor in wet CO₂ (< 3% mol) seem insignificant to modify heat and mass transfer in the gas-phase burning.

4.2 Surface reactions

4.2.1 Oxide cap

One important observation obviously concerns the oxide cap with its size regression after formation in wet CO₂ and its stability in dry CO₂. The oxide cap size regression was already observed in [2,19], and this phenomenon was attributed to the chemical decomposition of alumina by liquid aluminum producing gaseous aluminum oxides ($\text{Al}_{(l)} + \text{Al}_2\text{O}_{3(l)} \rightarrow \text{AlO}$, Al_2O ...). The correspondence between the droplet temperature and the oxide cap regression rate was considered as a substantial argument in favor of this explanation. However, the opposite behavior of the oxide cap in dry CO₂ seems to call it into question. It is now clear

that the oxide cap regression especially occurs in water containing atmospheres ([2]: H₂O/O₂, H₂O/N₂, H₂O/Ar ; [19]: H₂O/CO₂, H₂O/CO₂/N₂ ; present work: wet CO₂). As it was suggested for the gas-phase burning, it is H₂ rather than H₂O which may have an effect on the oxide cap regression. In order to confirm this explanation, further experiments were carried out for Al droplets burning in CO₂/12% Ar, CO₂/21% He, and CO₂/5% H₂. It was observed that the oxide cap size does not vary with the addition of both inert gases, whereas it decreases in the presence of H₂. This comparison with argon and helium definitely demonstrates the fundamental role of hydrogen in the oxide cap regression process. Now one question remains about the mechanism in which hydrogen acts. First, it can be stated that it is a chemical effect. Another possibility may be that H₂ increases the mass transfer of the gaseous aluminum oxides formed by the cap decomposition similarly to Al evaporating from the droplet surface. But helium which is also a light gas with equivalent transport properties does not promote the regression process. The essential difference between H₂ and He is that one is chemically active when the other is inert. Nevertheless, the chemical effect of hydrogen is quite speculative. Thermodynamically, H₂ has no real influence on the decomposition of alumina; the hydrogenated species which could be formed (AlH, AlOH) are insignificant. In fact, the effect of hydrogen rather looks like a catalytic effect because small amounts of H₂ suffice to remove the oxide cap. Another detail suggests that the adsorption of H₂ on the Al droplet surface is probably the key mechanism. As illustrated in Figure 9, the time delay of the carbon ejection is longer for H₂O or H₂ containing atmospheres than for H₂O or H₂ free ones, which indicates that the presence of hydrogen slows down the carbon dissolution process. This is an important point because the carbon dissolution results from the dissociative adsorption (chemisorption) of CO at the droplet surface; the quite linearity between the time delay of ejection (t_{sat}) and the initial droplet diameter (d_0) confirms that heterogeneous kinetics controls these surface reactions. It was shown that oxygen is also dissolved, but in lower

quantities than carbon (% mol C=18-23; % mol O=8-10). Accordingly, the non-dissolved part of oxygen coming from CO is either gasified as aluminum oxides (AlO, Al₂O), or used for producing liquid alumina (Al₂O₃). For this last situation, the oxide cap evolution may be considered as a competition between the decomposition process (mass loss) and the oxygen contribution coming from CO (mass gain). The adsorbed hydrogen may prevent this oxygen contribution so that the cap decomposition would be higher and lead to the regression process.

4.2.2 Carbon ejection and fragmentation processes

The other important surface phenomenon is the carbon ejection. As observed with the camera, this is closely related to the presence or the absence of the oxide cap. In wet CO₂, the oxide cap is completely removed, and the carbon coating does not interact with other phases at the droplet surface. Therefore, no new combustion regime occurs even with the constant laser heating because carbon is a powerful refractory material which cannot be liquefied at such temperature and pressure conditions, and which prevents direct surface reactions between Al and CO₂. Obviously, some porosity may exist in the carbon coating and the diffusion of oxidizers or aluminum through carbon is also possible. However, such phenomenon is considered as insignificant because characteristic diffusion time is longer than typical burning time. The sudden expulsion or expulsion attempt of particles from the droplet is not clearly understood. These expulsions seem to result from gasification process inside the droplet rather than mechanical deformations. One gas source is dissolved hydrogen which has been identified previously in unburnt residues for water containing atmospheres [2,19]. In dry CO₂, the oxide cap is still there, and the carbon ejection process is longer than in wet CO₂. To describe this situation, the Al-O-C system must be considered through the Al₂O₃-Al₄C₃ phase diagram (Figure 10). Indeed, the oxide cap is also able to dissolve carbon up to 23% mol at T=2600 K (≈55% mol Al₄C₃). Nevertheless, the carbon dissolution process does not consist in a direct surface reaction between Al₂O₃ and CO; carbon has first to dissolve in liquid

aluminum, and then migrate through the Al/Al₂O₃ interface. At the carbon saturation limit in Al ($x_C=0.23$ at $T=2600$ K), the dissolution of carbon in the oxide cap continues which allows slowing down the carbon ejection at the surface, implying longer times of coating. The interactions between the oxide cap and the carbon coating differ from that observed between the cap and solid AlN [2]. In the first steps of the carbon growth, the two phases do not mix at collision. This fact suggests that either the oxide cap is already saturated in carbon and cannot dissolve it anymore, or the liquid cap cannot easily wet the solid phase. The second proposition seems more realistic because the interactions finally occur when the oxide cap is completely surrounded by carbon. Accordingly, the forced wetting process promotes the conversion of the carbon coating into an aluminum oxycarbide phase. This is crucial because the oxycarbide can be melted contrary to carbon; the overheated surface due to the laser breaks up in small liquid caps which free aluminum just below and allows to establish a new combustion regime. Such a regime is characterized by sudden deformations and fragmentation of the droplet (Figure 3, Figure 4). In previous works, fragmentation generally occurred for Al burning in O₂ containing atmospheres for $x_{O_2}>0.2$ [1,4,8,10,11,12,14], and was related to particle disintegration at boiling because of this high energetic oxidizer. However, the droplet temperature does not reach the boiling point ($T=2790$ K) in our experiments. Fragmentation was also observed in presence of other gaseous species such as CO₂ or N₂ [3,4,13,14]. In that case, it may result from the violent expulsion of gases produced by the decomposition reaction of aluminum oxycarbide or oxynitride phases: $Al_xO_y(C,N)_z \rightarrow Al_2O_3 + (CO, N_2)$ [3]. The gasification as source of fragmentation corresponds to our own observations and analyses. Indeed, the XRD analysis shows that the unburnt residues which are heated again for long times with bubbles breaking up at the surface (Figure 5) mostly contains alumina, and no carbonated phases. In fact, carbon which has been dissolved in significant amounts during the gas-phase burning is progressively

substituted by oxygen during the second combustion regime (Table I, $\text{Al}_4\text{C}_3 \rightarrow \text{Al}_4\text{O}_4\text{C} \rightarrow \text{Al}_2\text{O}_3$). Carbon is ejected from the droplet surface as CO in bubbles which explains why there is no flame at the bubble breakdown (no reaction between CO and CO_2). The formation of CO inside the droplet would cause these sudden increases of volume and lead to fragmentation.

4.3 Synthesis: a new model of Al burning

The present results allow the detailed description of various processes occurring during the combustion of aluminum droplets in wet and dry CO_2 . Figure 11 offers a qualitative model of Al burning and summarizes the possible combustion regimes. In the first stage of the burning process, combustion is classically controlled by gas-phase heat and mass diffusion mechanisms. This regime has been largely observed, and its characterization has been offered in terms of burning rates or times by applying d^2 -law or d^n -law models. The main contribution of the present work is the demonstration of the crucial role played by carbon dissolution during this gas-phase burning which was also described for submillimetric particles [20], and which completely changes the combustion regime. The carbon ejection at the droplet surface resulting from the carbon saturation in liquid aluminum and from the constant regression of the droplet size, occurs inevitably (as soon as carbon dissolves) and stops Al vaporization. A new stage of burning starts and depends on the presence or the absence of the oxide cap when carbon is ejected. With no oxide cap, the carbon encapsulates the droplet and prevents any surface reactions because of its refractory properties; in that case, combustion may be considered as definitely stopped. With an oxide cap, carbon transforms into an aluminum oxycarbide coating which can be melted and which allows direct surface reactions between Al and CO_2 . These reactions result in the slow oxidation of the droplet and the gradual elimination of dissolved carbon by producing CO. During this process, the internal gasification of CO may also cause the fragmentation of the droplet.

The behavior of carbon in the combustion of aluminum droplets merits full considerations. Indeed, at the beginning and the end of burning, no carbon is present in the initial droplet ($\approx \text{Al}$) nor in the final residue ($\approx \text{Al}_2\text{O}_3$); from a thermodynamic point of view, the chemical reaction $2 \text{Al} + 3 \text{CO}_2 \rightarrow \text{Al}_2\text{O}_3 + 3 \text{CO}$ gives a quite good approximation of the global energetics of Al/CO₂ combustion. However, this simplification occults the cycle of carbon, first dissolved and then ejected from the droplet, and misses the fundamental role of heterogeneous kinetics (adsorption, catalysis). In our experiments, the carbon ejection occurs for $d=0.6-0.8 \cdot d_0$, which means that between 50% and 80% of the aluminum mass is consumed during the first (gas-phase) burning stage. Accordingly, a significant fraction of Al is still available for the second burning regime. The transposition of such processes to the solid propellant conditions (submillimetric particle sizes, high pressures) was discussed previously [19], and it was argued that there are no reasons to neglect them. Indeed, the carbon dissolution process was already described for 250 μm diameter Al particles burning in pure CO₂ by [20], and oxycarbide phases were found by [4] in submillimetric particle residues. For micrometric particles, it is rather a lack of analyses than an absence of the carbon dissolution, because it is experimentally difficult to observe in situ the carbon ejection process, and no carbon quantification has been carried out on the residues. Nevertheless, one question remains about the nature of the second combustion regime in terms of carbonated phase forming at the droplet surface (carbon encapsulation or oxycarbide coating). Obviously, this regime depends on the presence or not of the oxide cap. In experimental studies simulating the propellant conditions [9], the oxide cap is generally observed which suggests the formation of the oxycarbide coating, its melting by the hot ambient gases, the surface oxidation and the carbon regeneration into CO.

Therefore modeling of Al droplet combustion in CO₂ [24] necessitates the introduction of these new mechanisms, increasing its complexity. For example, the second burning regime

duration seems to be very difficult to estimate. Nevertheless, the gas-phase burning time taking into account the carbon dissolution process (first combustion stage) may be evaluated, and this has to be investigated in future work.

5 Conclusions

This study on the combustion of aluminum droplets in wet (3% mol H₂O) and dry CO₂ has demonstrated the existence of a second burning regime occurring after the carbon ejection process. The nature of this new regime depends on the presence or the absence of the oxide cap on the droplet surface which depends itself on the presence or the absence of hydrogen in the gaseous atmosphere. In fact, during the gas-phase burning, heterogeneous kinetics discreetly prepare the advent of the next combustion regime, through chemisorption between the Al surface and the gaseous products coming from the flame, especially CO for the carbon dissolution, and H₂ for the oxide cap regression. Then, during the second stage of burning, surface reactions are predominant and promote the gradual oxidation of the droplet at the detriment of dissolved carbon which is regenerated as CO. This gasification process is proposed to be an important source of fragmentation.

Acknowledgments

The authors acknowledge the support of the CNRS, the Conseil Régional Centre, and the Fonds Social Européen, Objectif 2, 2000-2006.

References

1. R. Friedman, A. Maček, *Combust. Flame*, 6 (1962) 9-19.
2. V. Sarou-Kanian, J.C. Rifflet, F. Millot, G. Matzen, I. Gökalp, *Proc. Combust. Inst.*, 30 (2) (2004) 2060-2067.
3. J.L. Prentice, *Combust. Sci. and Tech.*, 1 (1970) 385-398.
4. J.L. Prentice, Aluminum droplet combustion: Rates and mechanisms in wet and dry oxidizers, Naval Weapons Center, Report No TP 5569, 1974.
5. E.L. Dreizin, *Combust. Flame*, 105 (1996) 541-556.
6. A. Zenin, G. Kusnezov, V. Kolesnikov, AIAA paper 99-0696 (1999).
7. A. Zenin, G. Kusnezov, V. Kolesnikov, AIAA paper 2000-0849 (2000).
8. A. Zenin, G. Kusnezov, V. Kolesnikov, AIAA paper 2001-0472 (2001).
9. J.C. Melcher, R.L. Burton, H. Krier, *J. Prop. Power*, 18 (3) (2002) 631-640.
10. A. Davis, *Combust. Flame*, 7 (1963) 359-367.
11. C.M. Drew, A.S. Gordon, R.H. Knipe, *Heterogeneous Combustion, Progress in Astronautics and Aeronautics*, Vol. 15, 1964 pp. 17-39.
12. D.K. Kuehl, *AIAA Journ.*, 3 (12) (1965) 2239-2247.
13. A. Maček, *Proc. Combust. Inst.*, 11 (1967) 203-217.
14. P. Bucher, F.L. Yetter, F.L. Dryer, E.P. Vicenzi, T.P. Parr, D.M. Hanson-Parr, *Combust. Flame*, 117 (1999) 351-361.
15. C.K. Law, *Combust. Sci. and Technol.*, 7 (1973) 197-212.
16. P. Bucher, F.L. Yetter, F.L. Dryer, T.P. Parr, D.M. Hanson-Parr, *Proc. Combust. Inst.*, 27 (1998) 2421-2429.
17. J.L. Prentice, L.S. Nelson, *J. Electrochem. Soc.*, 115 (8) (1968) 809-812.
18. E.L. Dreizin, *Combust. Flame*, 117 (1999) 841-850.

19. V. Sarou-Kanian, J.C. Rifflet, F. Millot, E. Véron, T. Sauvage, I. Gökalp, *Combust. Sci. and Tech.*, submitted.
20. S. Rossi, E.L. Dreizin, C.K. Law, *Combust. Sci. and Technol.*, 164 (2001) 209-237.
21. E.Y. Shafirovich, U.I. Goldshleger, *Proc. 22th Int. Pyrotechnics Seminar*, (1996).
22. V. Sarou-Kanian, J.C. Rifflet, F. Millot, *Int. J. Thermophys.*, 26 (4) (2005).
23. C. Qiu, R. Metselaar, *J. Am. Ceram. Soc.*, 80 (1997) 8:2013-2020.
24. M.K. King, *Proc. Combust. Inst.*, 17 (1979) 1317-1328.

Tables

Experiments	Reheat	Burning stages	Phases			
			Al	Al ₄ C ₃	Al ₄ O ₄ C	Al ₂ O ₃
Wet CO ₂	No	GP	++	++	+	
Dry CO ₂		GP/SR-L	++	++	+	
Dry CO ₂	Yes	SR-L	++	+	++	
Dry CO ₂	Increasing times ↓	SR-L	+	+	+	+
Dry CO ₂		SR-B			+	++
Dry CO ₂		SR-B				++
Dry CO ₂		SR-B				++

Table I : XRD analysis of unburnt residues in wet and dry CO₂ and for different thermal treatments. Burning stages: GP = gas-phase; SR-L = surface reactions with liquefaction of the coating ; SR-B = surface reactions with bubbles only. Phases (semi-quantitative), + : significant, ++ : major.

Figures captions

Figure 1 : Ignition and gas-phase burning of aluminum droplets in wet and dry CO₂.

Figure 2 : Carbon ejection process, and expulsion and aborted expulsion attempt of particles for an aluminum droplet burning in wet CO₂.

Figure 3 : Carbon ejection process, liquefaction of the coating, and sudden deformations of an aluminum droplet burning in dry CO₂.

Figure 4 : Fragmentation of an aluminum droplet burning in dry CO₂.

Figure 5 : Effect of long time reheat for an aluminum droplet burning in dry CO₂.

Figure 6 : Pyrometric signals of aluminum droplets burning in wet (black line) and dry CO₂ (grey line). (1) complete covering, (2) first islands.

Figure 7 : Reduced squared diameter as a function of reduced time for aluminum droplets burning in wet (●) and dry (□) CO₂.

Figure 8 : Squared diameter as a function of time for oxide caps in wet (●) and dry (□) CO₂.

Figure 9 : Time delay of carbon ejection as a function of the initial droplet diameter in several CO₂ containing atmospheres. □: CO₂/H₂O ($x_{\text{CO}_2} > 0.8$), ∇: CO₂/H₂, ●: dry CO₂, ▲: CO₂/He, ◆: CO₂/Ar.

Figure 10 : Pseudo-binary phase diagram of the Al₂O₃/Al₄C₃ system from [23].

Figure 11 : Synthesis of the Al burning in CO₂.

Figures

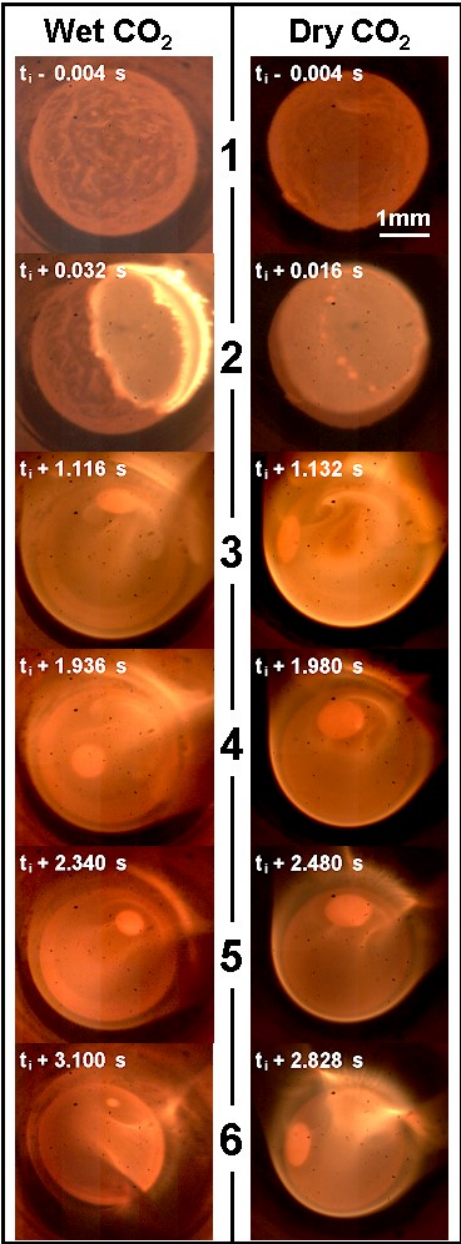


Figure 1

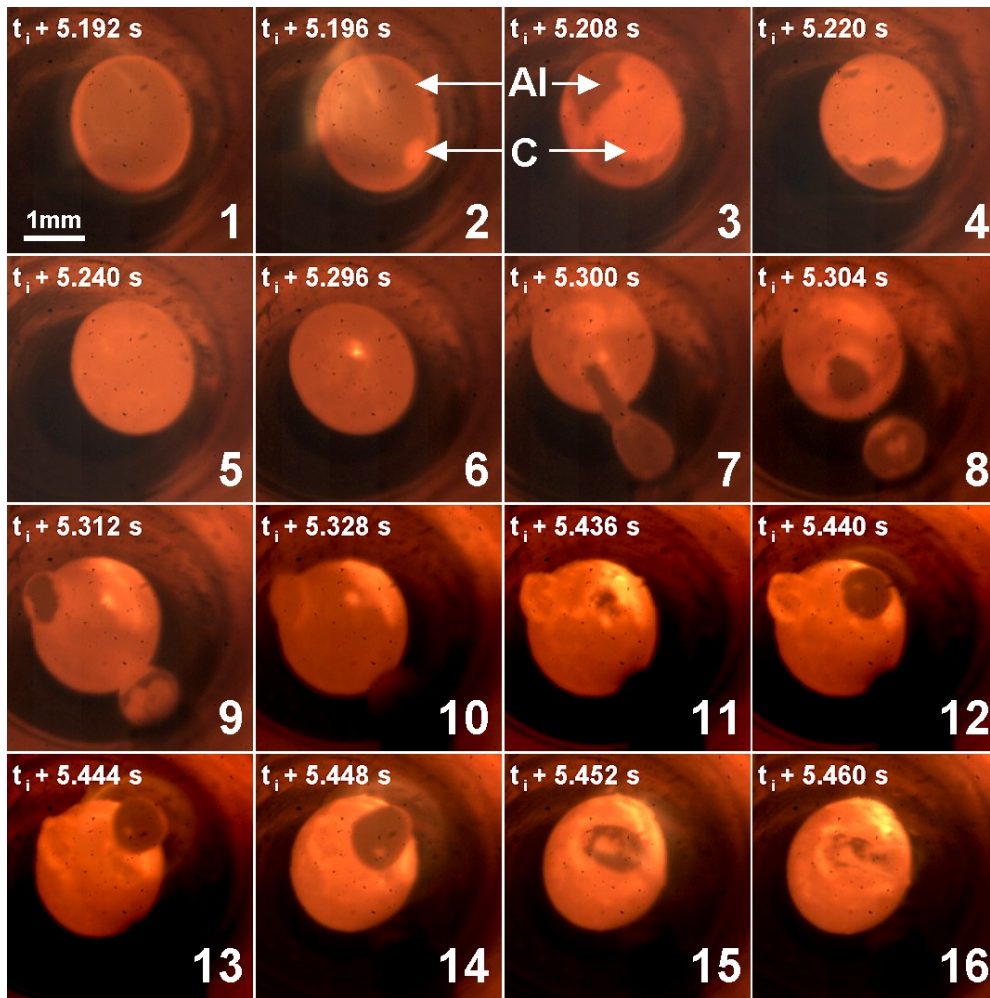


Figure 2

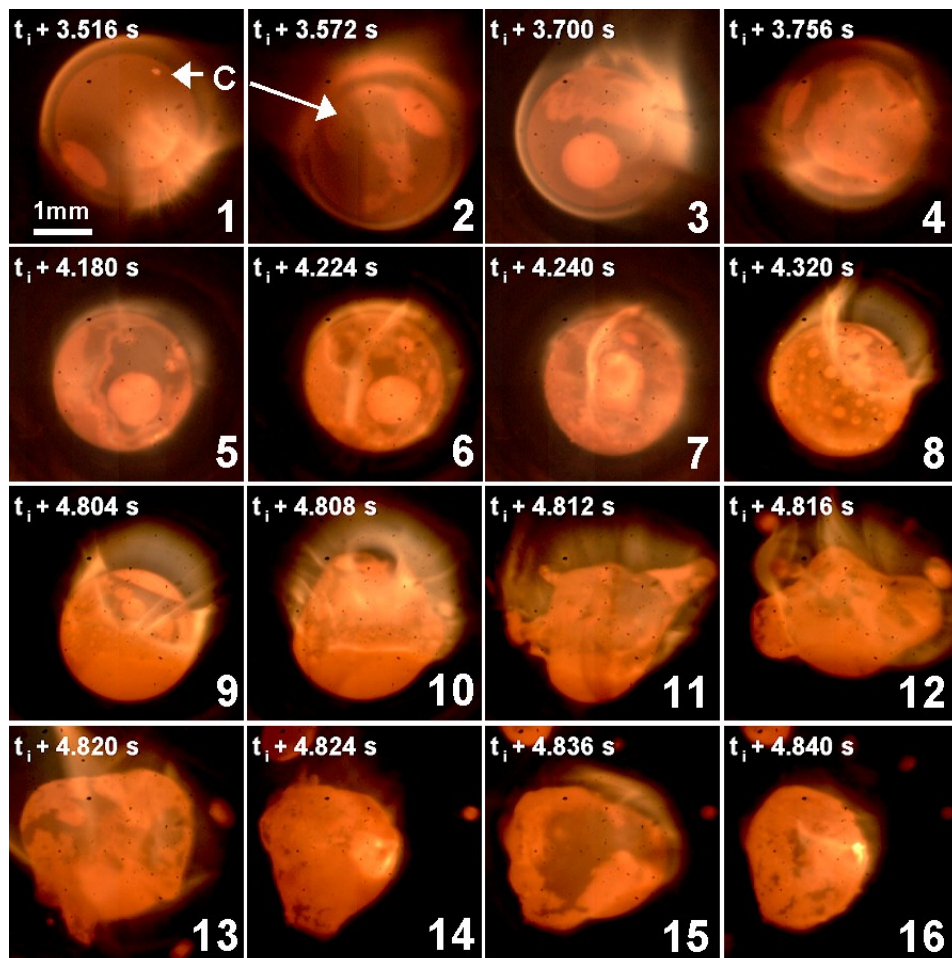


Figure 3

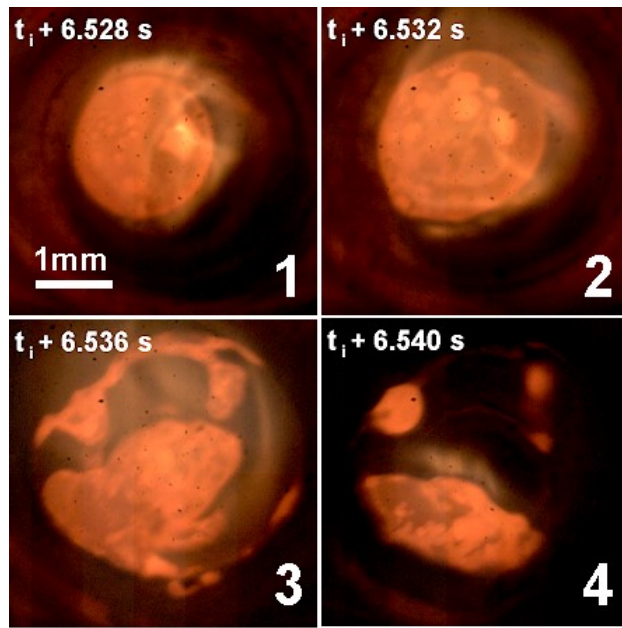


Figure 4

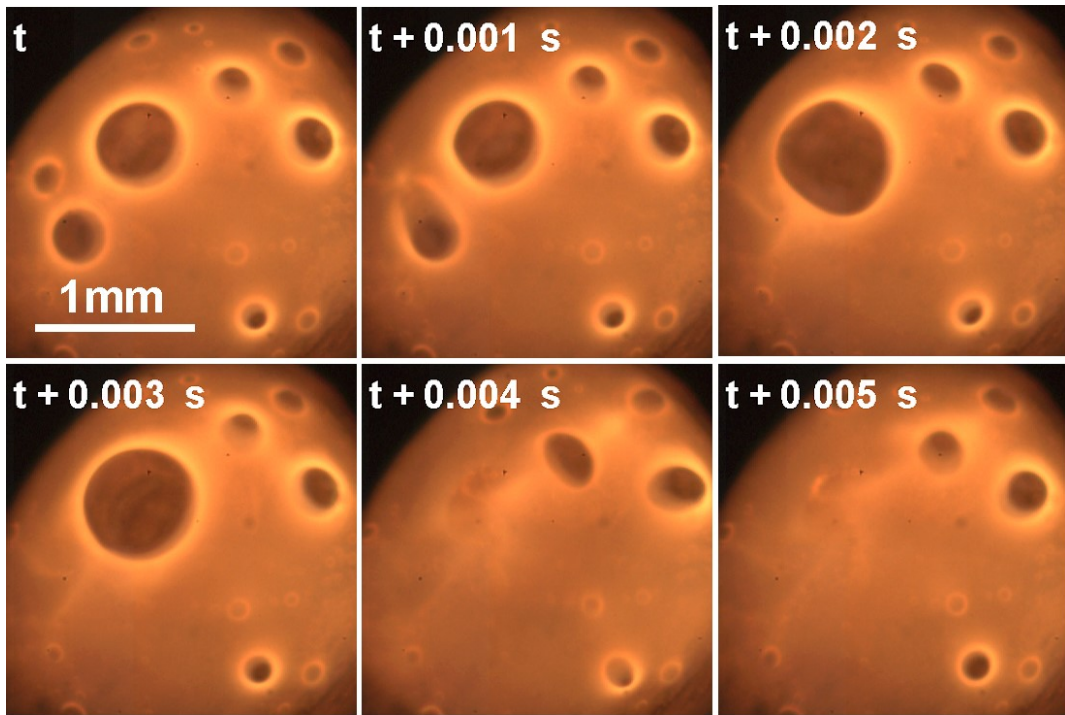


Figure 5

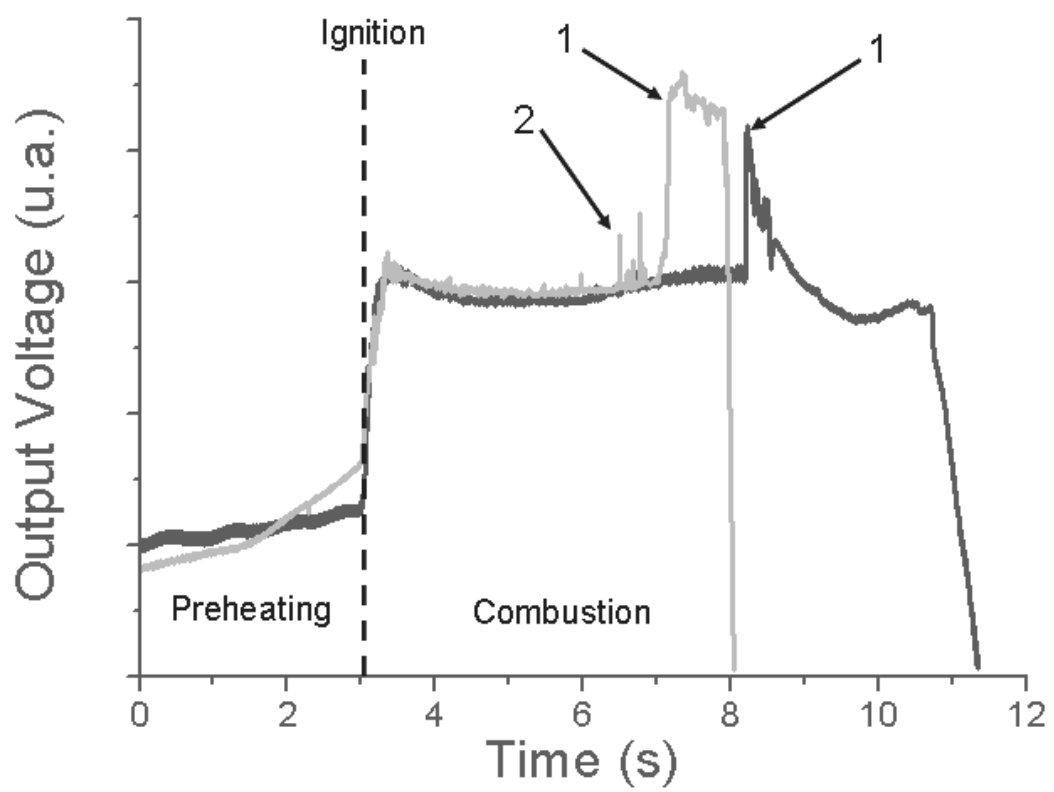


Figure 6

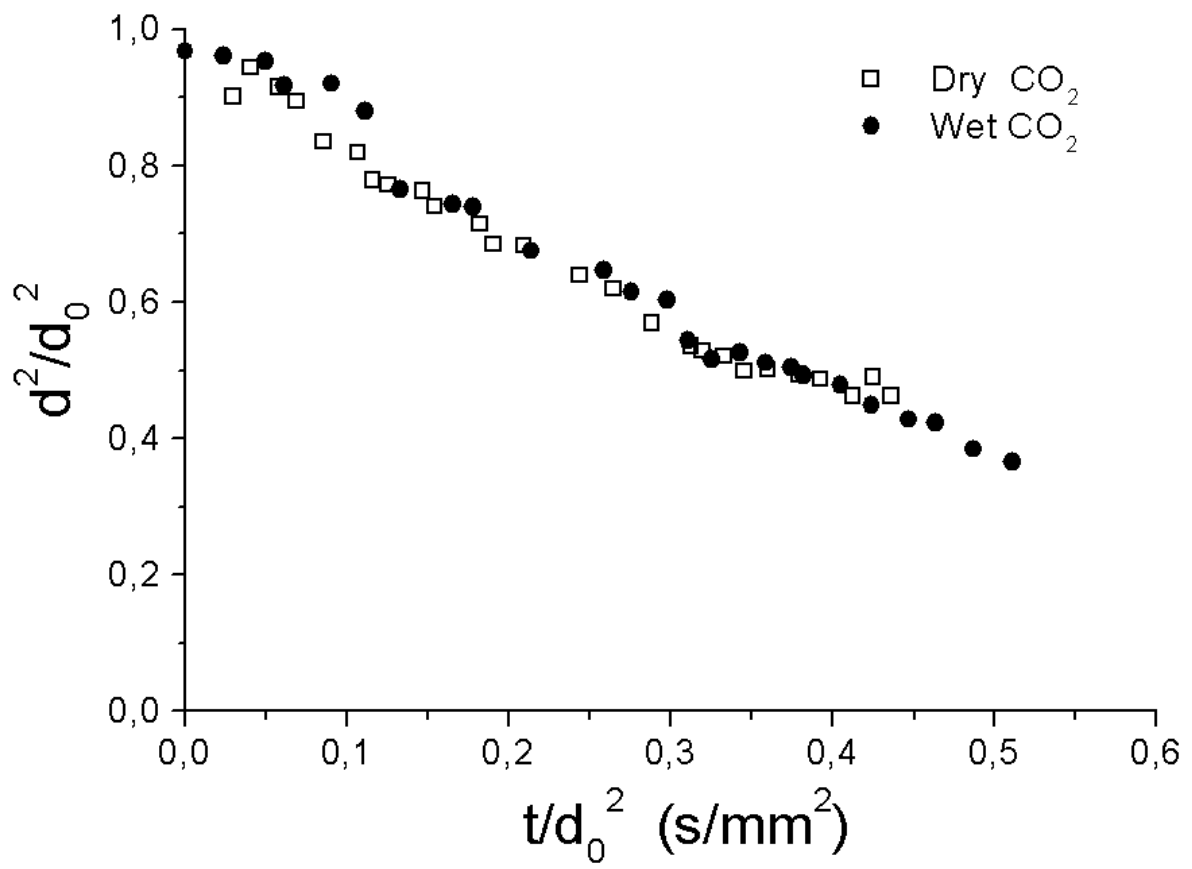


Figure 7

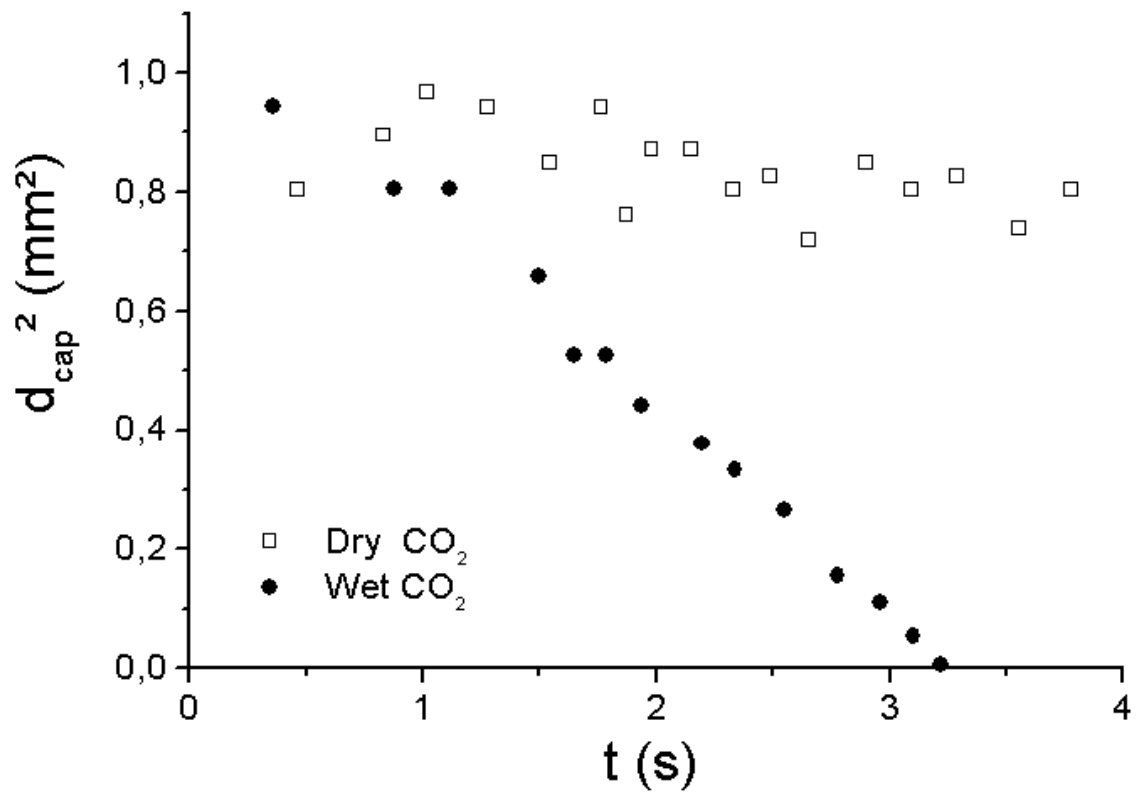


Figure 8

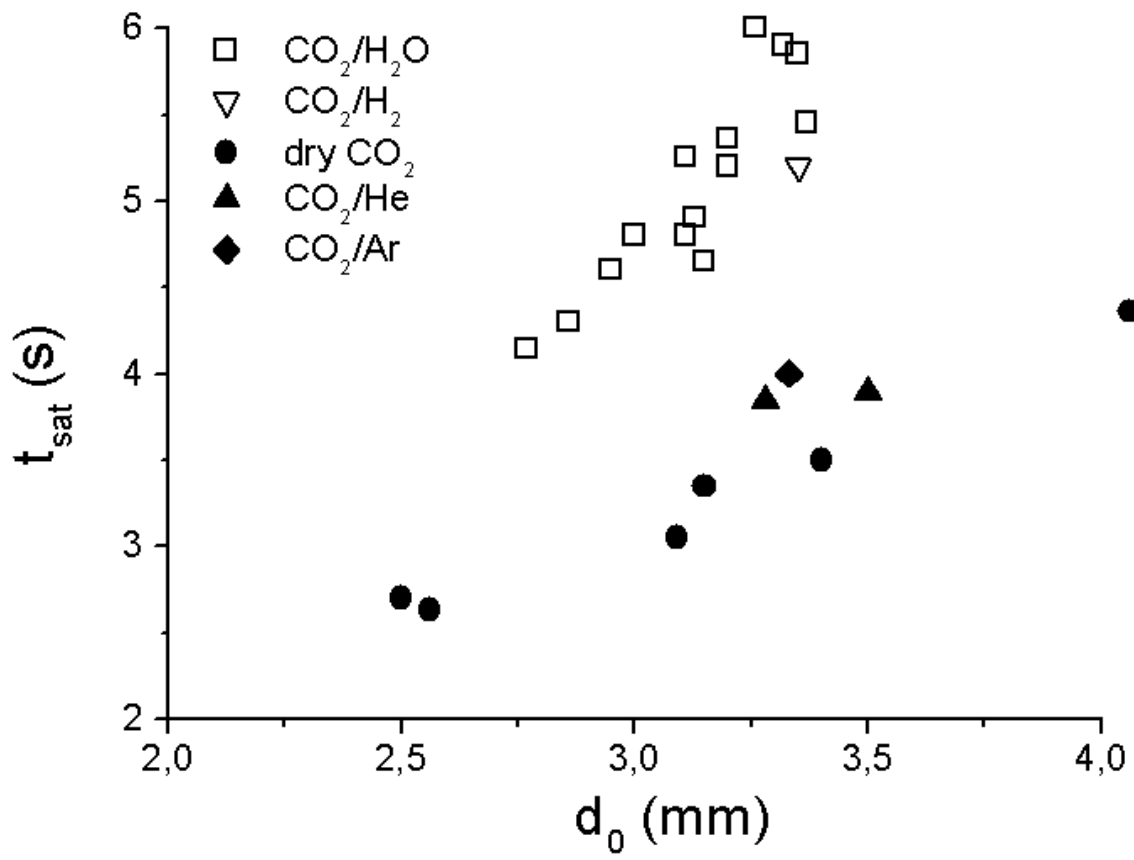


Figure 9

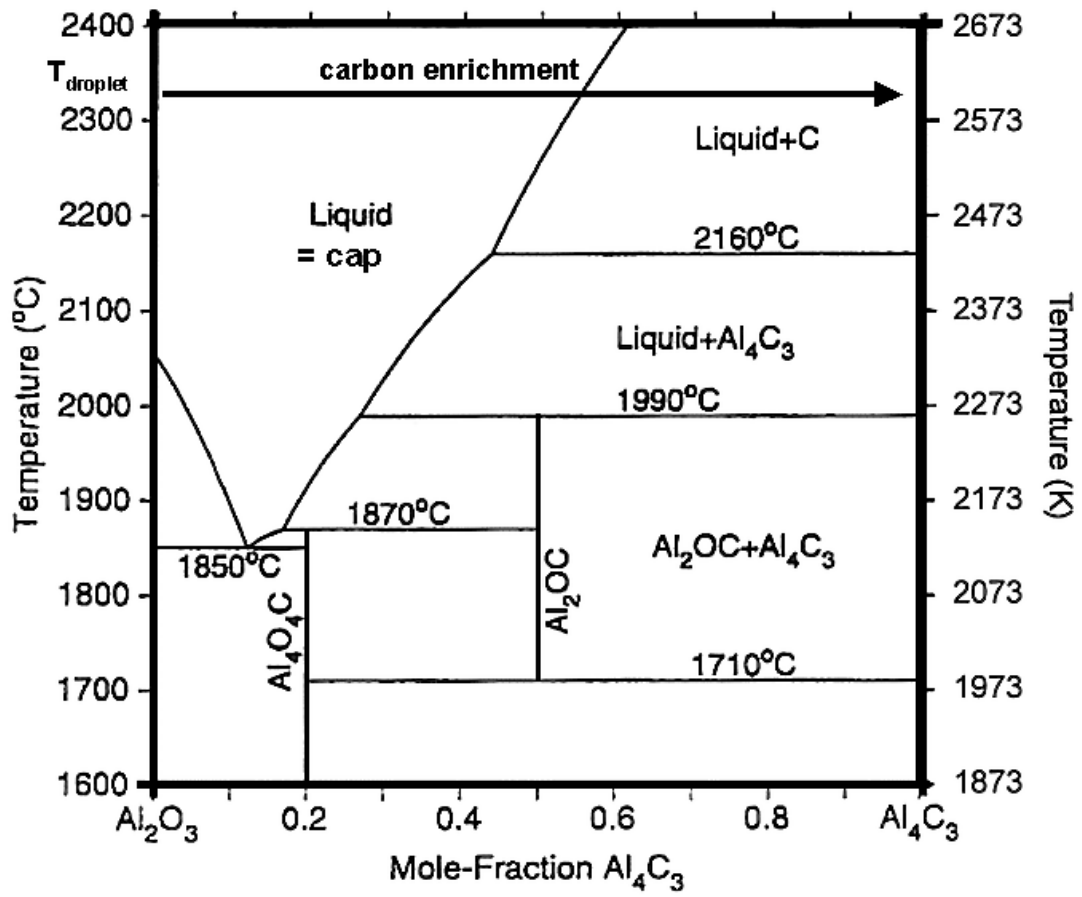


Figure 10

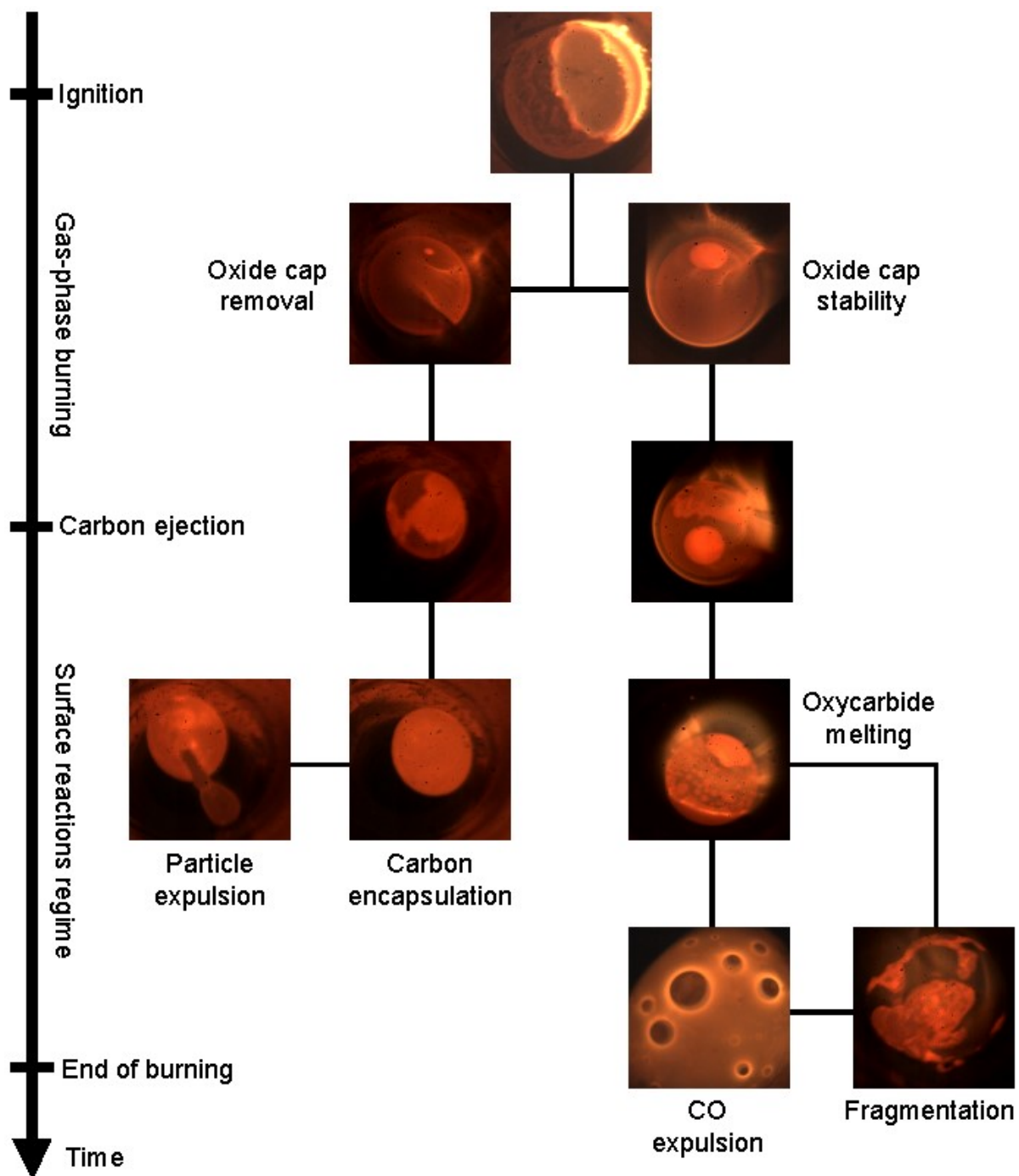


Figure 11